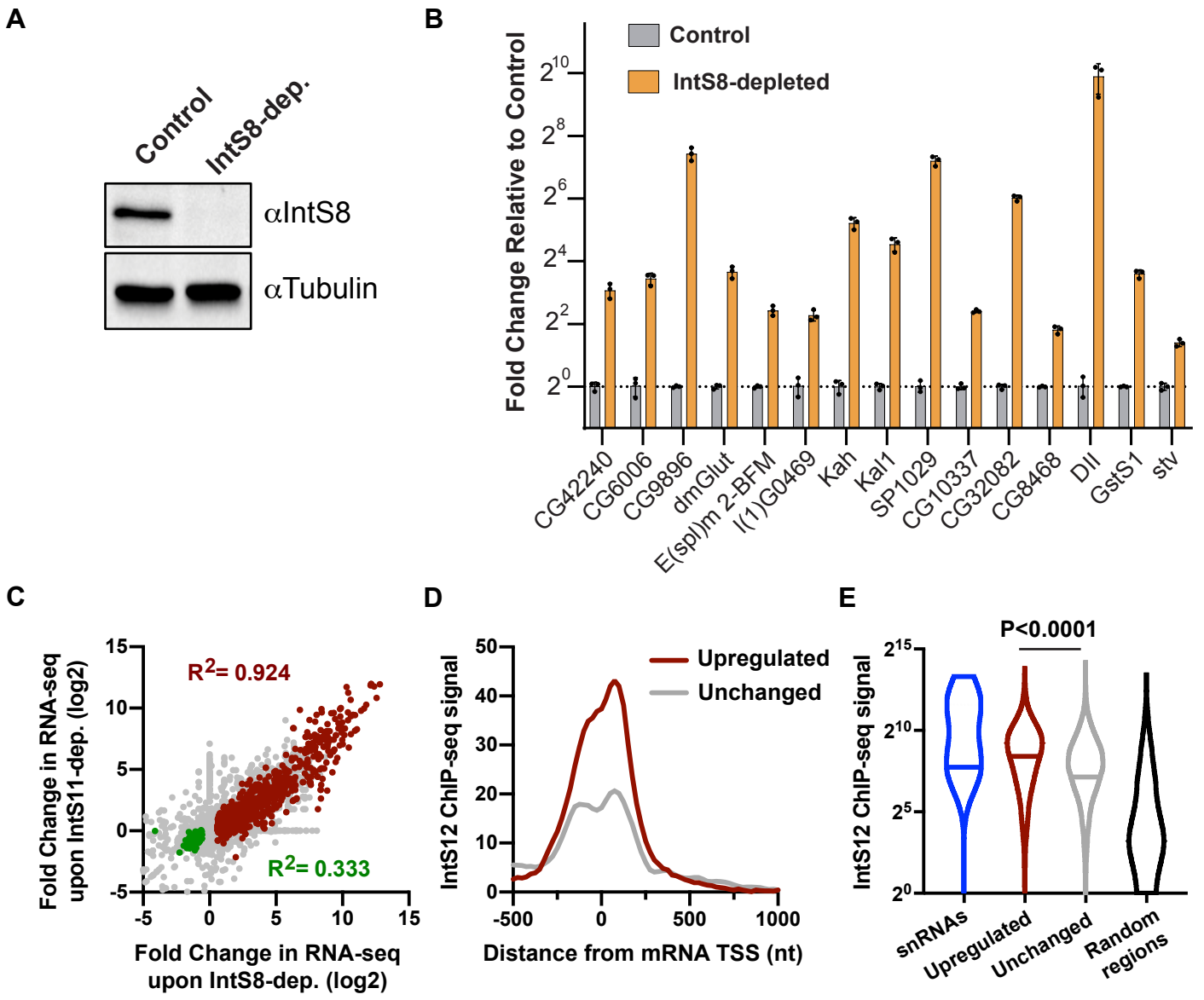

Figure S1. Related to Figure 1. Depletion of IntS8 causes activation of genes bound by the Integrator complex

(A) Western blot analysis of Drosophila DL1 cell lysates from cells treated with either control dsRNA (β-gal) or dsRNA targeting IntS8. Lysates are probed for endogenous IntS8 or Tubulin.

(B) RT-qPCR analysis of selected genes identified to be upregulated upon IntS8 depletion using RNA-seq. Results are shown from biologically independent replicates, depicting averages and standard deviations (mean +/- SD, N=3).

(C) Comparison of fold changes in RNA-seq signals between cells depleted of IntS8 and IntS11, the endonuclease containing subunit of Integrator. Pearson correlations are shown for genes upregulated (red) or downregulated (green) upon depletion of IntS8.

(D) Composite metagene analysis of IntS12 ChIP-seq reads around promoters of mRNA genes upregulated (N=1009) or unchanged (N=8022) upon IntS8 depletion. Data are shown as average reads per gene in 25-bp bins.

(E) Promoter-proximal read counts for IntS12 ChIP-seq were summed around snRNAs (N=31), randomly selected regions (N=5000) or promoters upregulated or unchanged by IntS8 depletion, as in D. Violin plots depict the range of values, with median indicated by a line. P value calculated using a Mann-Whitney test.

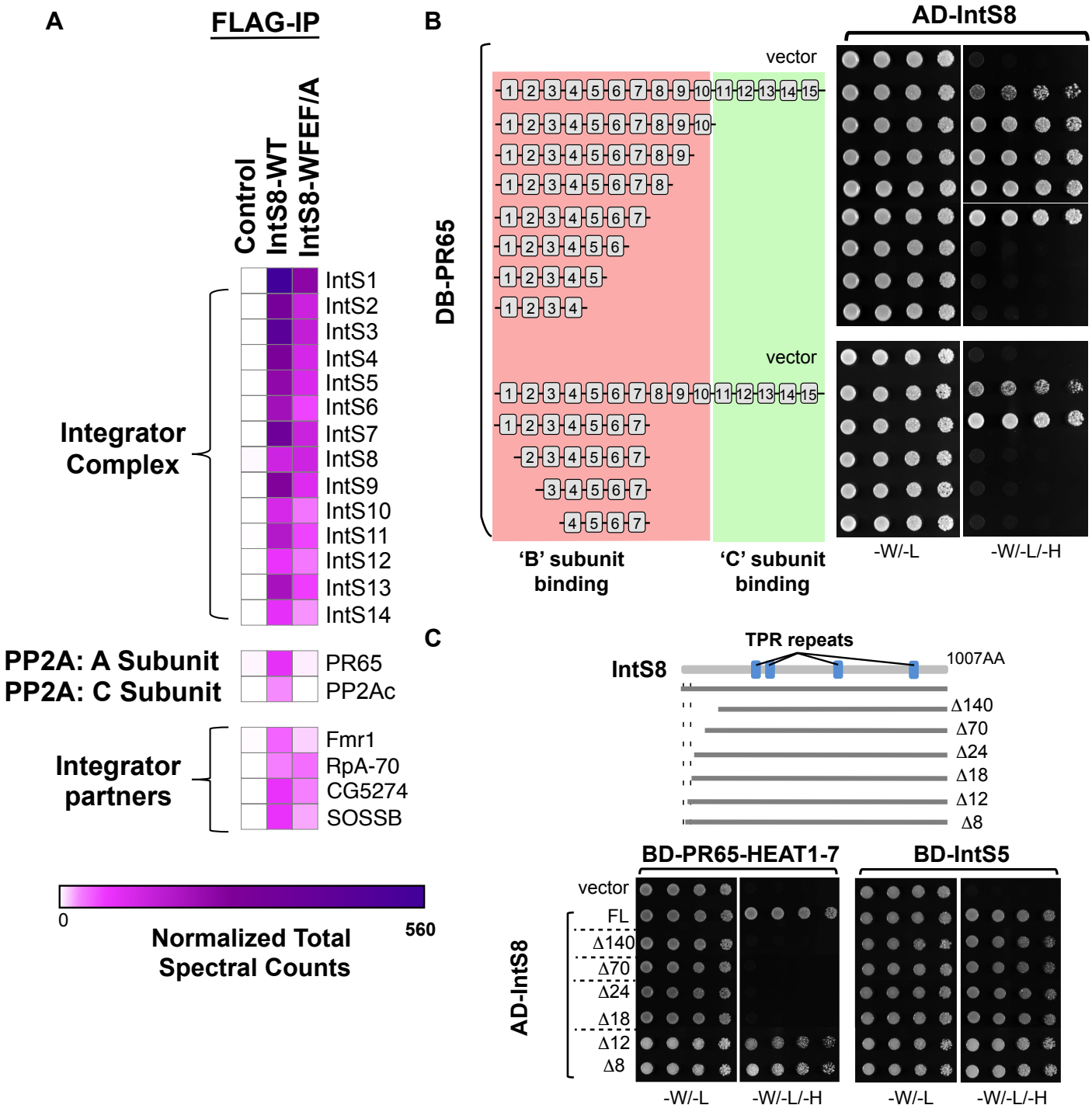

Figure S2. Related to Figure 2. IntS8 uses a conserved motif to associate with HEAT repeats 1-7 of PR65

(A) Heatmap generated from anti-FLAG purification of the indicated proteins, followed by LC-MS analysis. Results are quantified as average of triplicate measurements from purification and color grades represent normalized total spectral counts of each denoted protein. Notably, there is no enrichment over control of PP2A subunits associated with FLAG-IntS8-WFEF/A. There is also no significant difference in Integrator subunit association between either IntS8 protein and comparable association with Integrator partners, none of which have been previously ascribed a function in termination.

(B) Results of yeast two-hybrid analysis where either full-length PR65 or deletion mutants are fused to the Gal4 DNA binding domain. These constructs were screened for interaction with IntS8, which is expressed as a fusion protein with the Gal4 activation domain. Empty vector is the negative control. The individual PR65 HEAT repeats are labeled and the domains of PR65 that bind the 'B' regulatory subunit or 'C' catalytic subunit are highlighted. Permissive plates lack leucine and tryptophan (-L/-W) to allow growth of plasmid-containing yeast whereas selective plates also lack histidine to screen for interaction (-L/-W/-H). Yeast are plated in five-fold serial dilutions.

(C) Results of yeast two-hybrid analysis where either PR65 HEAT repeats 1-7 or IntS5 is expressed as a fusion protein to the Gal4 DNA binding domain and screened against full-length IntS8 or N-terminal deletion mutants expressed as fusions to Gal4 activation domain (diagrammed in schematic above). Yeast are plated as described in panel B. Note that dotted lines reflect junction points of multiple yeast plates put together for ease of viewing. All plates were imaged at the same exposure and at the same time.

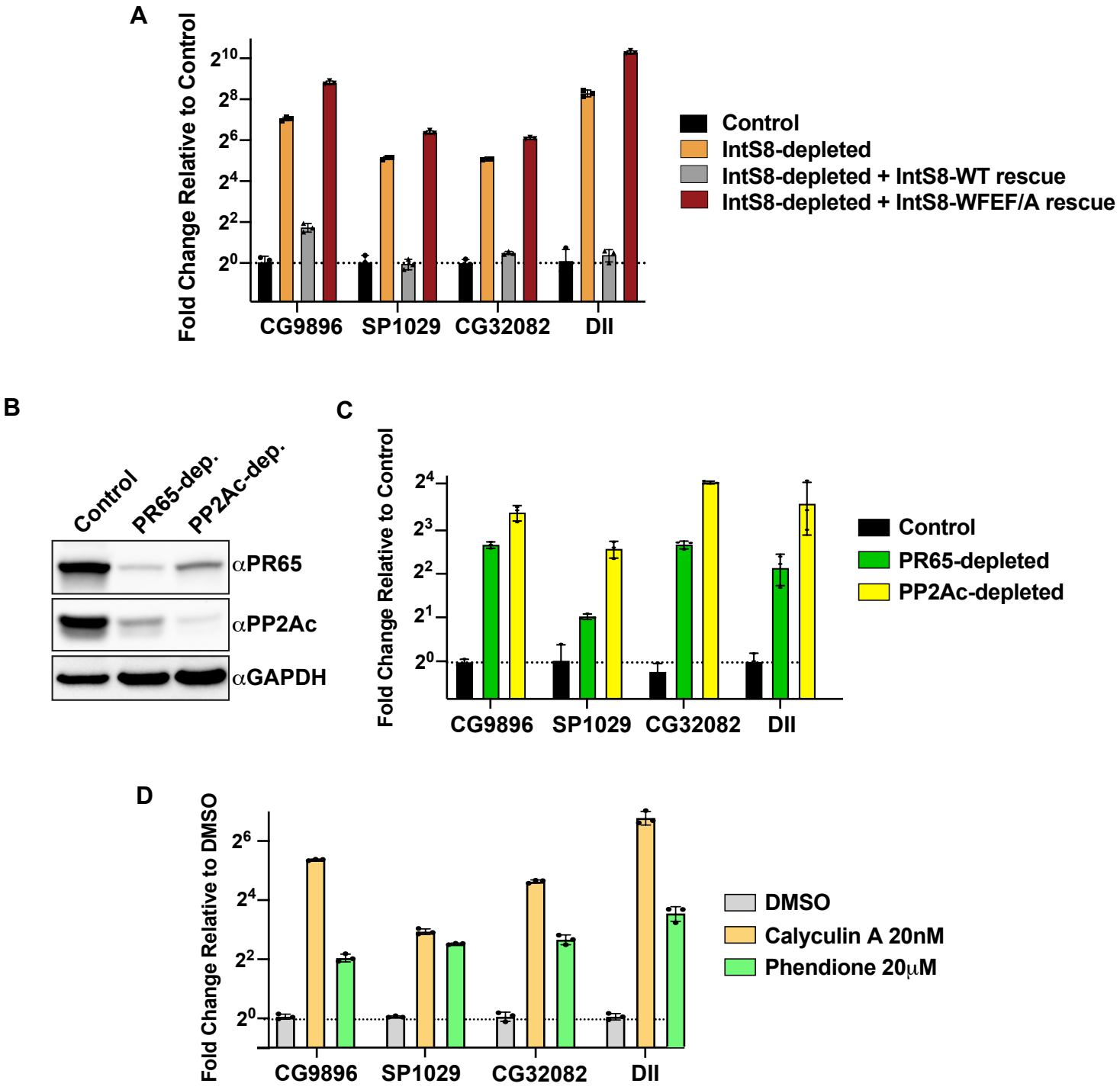

Figure S3. Related to Figure 3. Validation of RNA-seq analyses and comparison with PP2A inhibition.

(A) RT-qPCR was performed on total RNA isolated from DL1 cells treated with either control dsRNA (targeting β-galactosidase), dsRNA targeting IntS8 (IntS8-depleted), dsRNA targeting IntS8 where RNAi-resistant wild-type IntS8 was re-expressed (IntS8-depleted + IntS8-WT rescue), or dsRNA targeting IntS8 where RNAi-resistant WFEF/A IntS8 mutant was re-expressed (IntS8-depleted + IntS8-WFEF/A rescue). Results are shown from biologically independent replicates, depicting averages and standard deviations (mean +/- SD, N=3).

(B) Western blot analysis of DL1 cells treated with control dsRNA, dsRNA targeting PR65, or dsRNA targeting PP2Ac (Drosophila gene name *mts*). Effective depletion is observed as well as co-depletion likely due to heterodimeric interaction.

(C) RT-qPCR was performed on total RNA isolated from DL1 cells treated for 72 hours with either control dsRNA or dsRNA targeting PR65 or PP2Ac (*mts*) subunits of PP2A. Results are shown from biologically independent replicates, depicting averages and standard deviations (mean +/- SD, N=3).

(D) RT-qPCR was performed on total RNA isolated from DL1 cells treated for 24 hours or treatment with Calyculin A (20nM) or Phendione (20μM). Results are shown from biologically independent replicates, depicting averages and standard deviations (mean +/- SD, N=3).

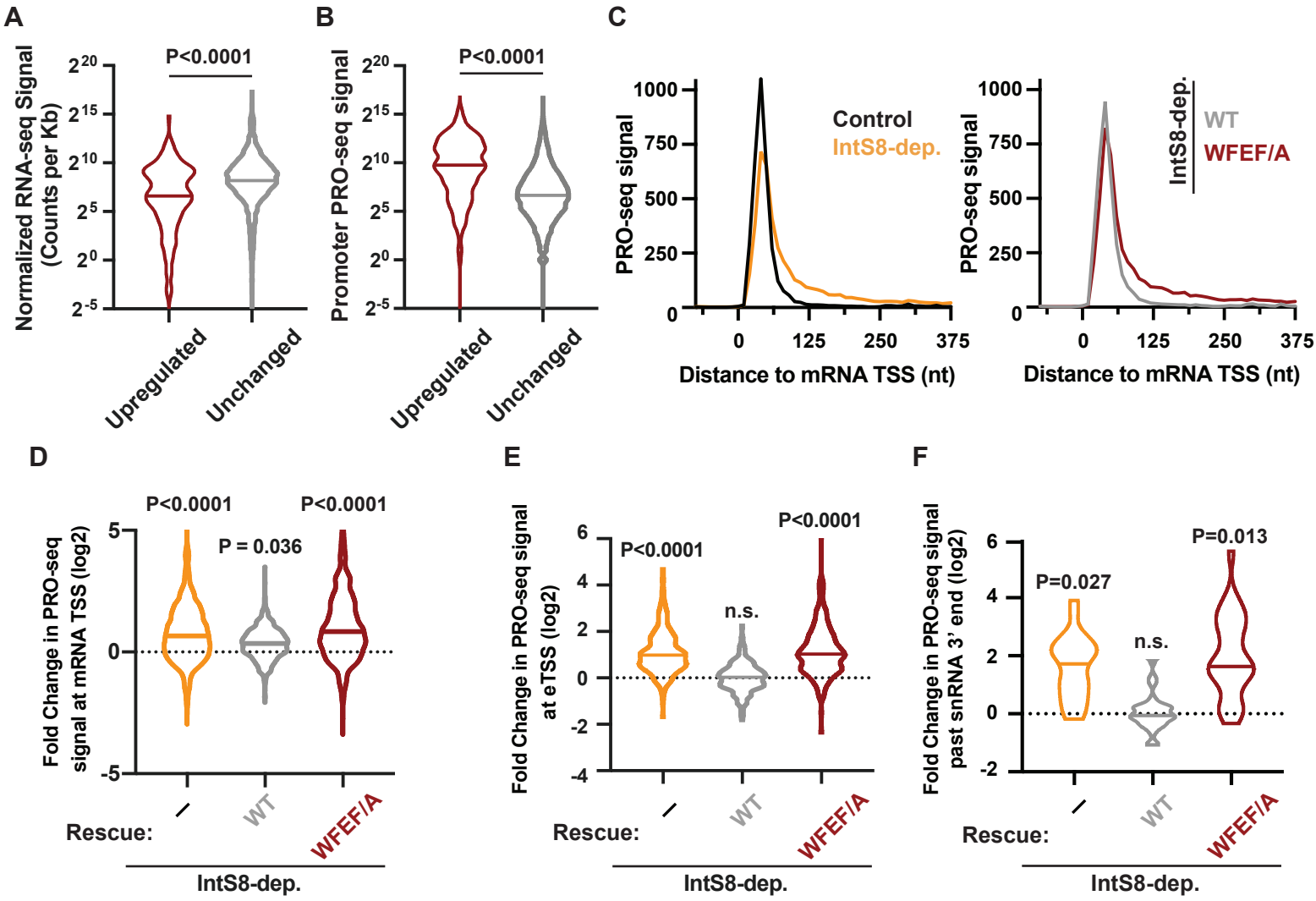

Figure S4. Related to Figure 4. Loss of IntS8-PP2A interaction abrogates Integrator-mediated termination. All violin plots in this figure show the range of values, with a line indicating median.

(A) Violin plots depict normalized RNA-seq counts (from control data shown in Figure 3) for upregulated (N=649) and unchanged (N=7182) genes. P value calculated using a Mann-Whitney test.

(B) Violin plots depict PRO-seq signal from control cells at mRNA promoters (TSS to +150 nt) for upregulated (N=649) and unchanged (N=7182) genes. P value calculated using a Mann-Whitney test.

(C) Average distribution of PRO-seq signal is shown at genes upregulated upon IntS8 depletion in RNA-seq (N=649) using 10-nt bins. The left panel shows control dsRNA compared to IntS8 dsRNA, treated as in Figure 3. The right panel shows IntS8 depletion rescued with transgenic WT IntS8 or IntS8 WFEF/A mutant.

(D) Violin plots depict the change in PRO-seq signal at 649 upregulated gene promoters, summing the PRO-seq read counts from the TSS to +150 nt downstream. P values calculated using a Kruskal-Wallis test with Dunn's multiple comparisons.

(E) Violin plots depict the change in PRO-seq signal at 228 IntS9-attenuated eTSSs (from +250 to +750 nt downstream; as defined in Elrod et al., 2019). P values calculated using a Kruskal-Wallis test with Dunn's multiple comparisons.

(F) Violin plots depict the change in PRO-seq signal downstream of 31 snRNA gene 3' ends (+1000 to +1500 nt from 3' end), measuring transcriptional read through for each treatment. P values calculated using a Kruskal-Wallis test with Dunn's multiple comparisons.

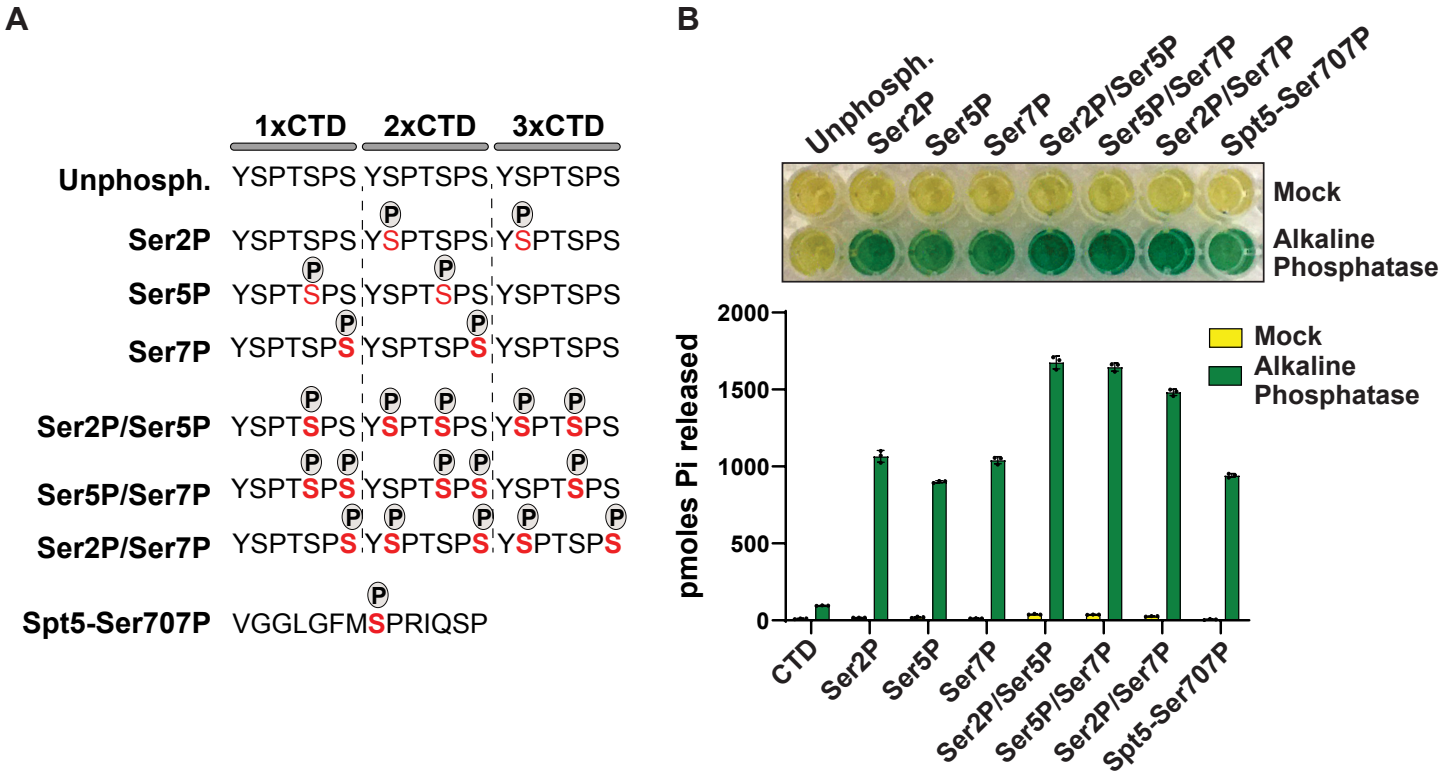

Figure S5. Related to Figure 5. All synthetic phospho-peptides can release orthophosphate upon treatment with alkaline phosphatase, as detected in the malachite green assay

(A) Schematic of synthetic peptides used for in vitro phosphatase assays.

(B) Results of malachite green assay where individual peptides shown in panel A were incubated with alkaline phosphatase or with identical buffer conditions but lacking enzyme (Mock). Representative colorimetric results are shown in the upper panel. Results from triplicate assays are quantified as picomoles of orthophosphate produced. Phosphate standards were used to calculate pmoles produced.

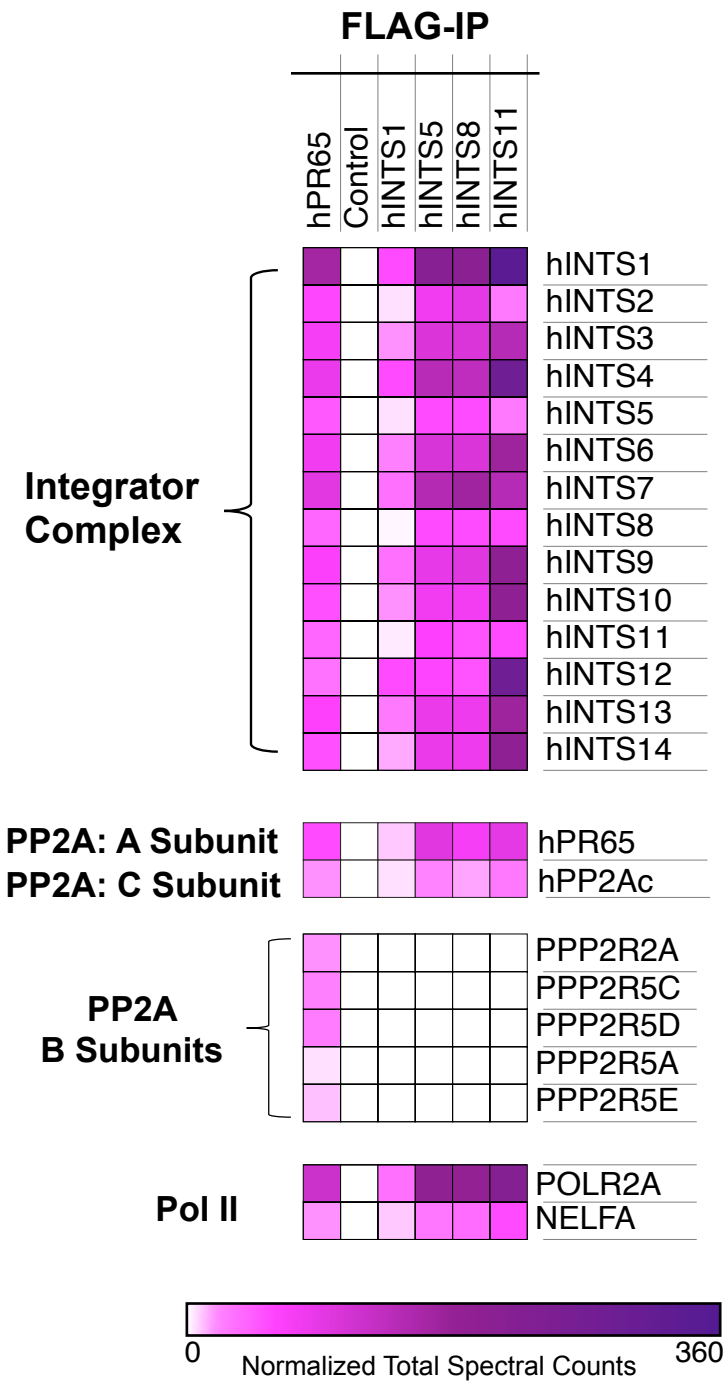

Figure S6. Related to Figure 6. Human Integrator Complexes contain PR65/PP2Ac but not PP2A B regulatory subunits

Heatmap derived from IP MS/MS analysis of FLAG immunoprecipitations from 293T cells harboring single FLAG epitope tags incorporated into the genomic regions encoding PR65, INTS1, INTS5, INTS8, and INTS11. Epitope tags were integrated using CRISPR/Cas9 genome-editing. Heatmaps reflect normalized spectral counts observed from analysis of samples performed in triplicate. 293T Control cells lack any exogenously expressed FLAG-tagged protein.

A

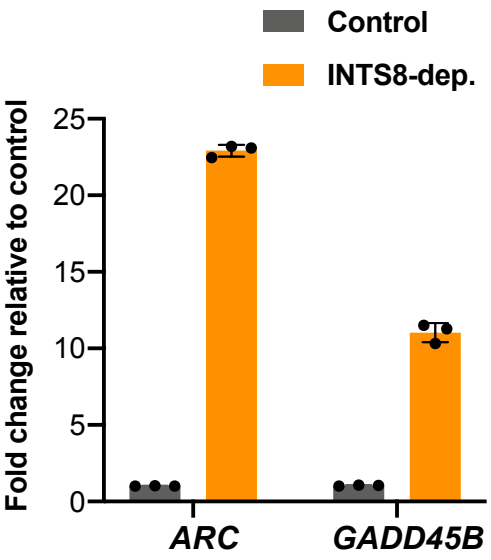

B

Upregulated genes upon INTS8-depletion

Top GO Molecular Function	Adjusted P value
Calcium signaling pathway	0.027
Parathyroid hormone synthesis, secretion and action	0.031
Neuroactive ligand-receptor interaction	0.033
MAPK signaling pathway	0.033
Pathways in cancer	0.039

Top KEGG pathways	Adjusted P value
MAPKK binding	0.024
Transmembrane Receptor Protein Kinase Activity	0.025
Transmembrane Receptor Protein Tyrosine Kinase Activity	0.045

Top INTERPRO domains	Adjusted P value
Basic-leucine zipper domain	0.0018
GPCR family 3, C-terminal	0.021
Serine-threonine/tyrosine-protein kinase, catalytic domain	0.022
Tyrosine-protein kinase, catalytic domain	0.022
EGF-like calcium-binding domain	0.022

C

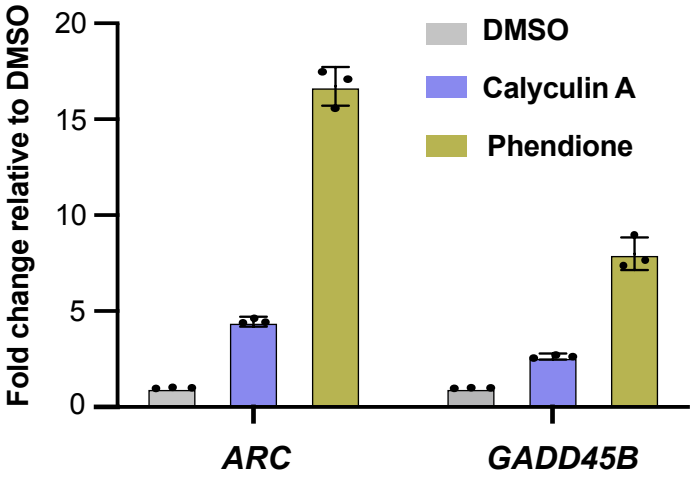

Figure S7. Related to Figure 7. Results for human INTS8 parallel those from the *Drosophila* system

(A) RT-qPCR validation of representative genes affected by Integrator in replicate 293T samples used in the preparation of RNA-sequencing libraries. Levels of Integrator target genes, *ARC* and *GADD45B*, were normalized to *ACTB* and the fold change upon INTS8 depletion is shown. (mean ± SD, N = 3).

(B) Gene Ontology analysis was performed on the 420 transcripts upregulated by INTS8 depletion in the RNA-seq assay. This corresponded to 420 unique genes that had defined Gene Ontology ID annotations in Enrichr. The top enriched functional categories, pathways and domains with adjusted P values < 0.05 are reported. No categories reached significance for the 53 downregulated genes.

(C) RT-qPCR measurement of representative genes affected by Integrator depletion in 293T cells demonstrates a similar effect upon PP2A pharmacological inhibition. Cells were treated for 24 hrs with either DMSO as a control, 4nM Calyculin A, or 2uM Phendione to inhibit PP2A. Levels of Integrator target genes, *ARC* and *GADD45B*, were normalized to *7SK* and the fold change upon PP2A inhibition is shown. (mean ± SD, N = 3).